Journal of Civil Structural Health Monitoring (2020) 10:235–250
https://doi.org/10.1007/s13349-020-00380-w

ORIGINAL PAPER

Dynamic structural health monitoring for concrete gravity dams based on the Bayesian inference

Giacomo Sevieri[1] · Anna De Falco[2]

Received: 22 May 2019 / Revised: 12 December 2019 / Accepted: 10 January 2020 / Published online: 4 February 2020

Abstract
The preservation of concrete dams is a key issue for researchers and practitioners in dam engineering because of the important role played by these infrastructures in the sustainability of our society. Since most of existing concrete dams were designed without considering their dynamic behaviour, monitoring their structural health is fundamental in achieving proper safety levels. Structural Health Monitoring systems based on ambient vibrations are thus crucial. However, the high computational burden related to numerical models and the numerous uncertainties affecting the results have so far prevented structural health monitoring systems for concrete dams from being developed. This study presents a framework for the dynamic structural health monitoring of concrete gravity dams in the Bayesian setting. The proposed approach has a relatively low computational burden, and detects damage and reduces uncertainties in predicting the structural behaviour of dams, thus improving the reliability of the structural health monitoring system itself. The application of the proposed procedure to an Italian concrete gravity dam demonstrates its feasibility in real cases.

Keywords Concrete dams · Structural health monitoring · General polynomial chaos expansion · Bayesian inference · Ambient vibrations · Operational modal analysis

1 Introduction

Concrete gravity dams are key to flood control, energy production, and the industrial and agricultural supply. Most of the existing concrete gravity dams were designed without considering their dynamic behaviour, and often their shapes were optimised according to static concepts. Moreover, the levels of reliability required to important infrastructures have been recently increased in order to meet the requests of communities for greater safety, also in light of the revaluation of some areas as seismic [1]. Together with the well-known issues related to the quantification of dam seismic safety [e.g., calibration of load-and-resistance-factor approaches, definition of limit states (LSs)] [2], this justifies the need for strategies that preserve such structures. In this context, the implementation of structural health monitoring (SHM) is very important, as it improves dam control and reduces the uncertainties involved in predicting their dynamic behaviour. However, SHM in dam engineering is very rare, mainly because of the large computational burden of predictive models, as discussed in Sect. 2.

Concrete dams are equipped with static monitoring systems, which usually record displacements at a few points in the dam body, basin levels and temperatures of the air and water. As shown in Sevieri et al. [3] this information can be used to calibrate predictive models of the structure for control purposes. However, in view of seismic events, dam control can be performed more effectively through dynamic monitoring systems. Sevieri et al. [4] show how ambient vibrations, and in particular their elaboration through operational modal analysis (OMA), can be successfully used to update the parameters of predictive models of concrete gravity dams' dynamic behaviour, thus reducing epistemic uncertainties.

This research work presents a new probabilistic ambient vibration-based SHM framework for real-time control of concrete gravity dams. The procedure exploits experimental modal characteristics deduced from the analysis of ambient

✉ Giacomo Sevieri
g.sevieri@ucl.ac.uk

1 Department of Civil, Environmental and Geomatic Engineering, University College London, Chadwick Building, Gower Street, London WC1E 6BT, UK

2 Department of Energy, Systems, Territory and Constructions Engineering, University of Pisa, Largo Lucio Lazzarino, 1, 56122 Pisa, Italy

vibrations via OMA. It consists of two phases: *Training* and *Detection*. The architecture of the system and the hierarchical statistical relationship between ambient vibrations, environmental measurements and model parameters enable analysts both to detect damage and to update the parameters of predictive models. Dynamic measurements thus provide structural control, thereby improving the prediction of the dam's structural behaviour. This latter is possible thanks to the Bayesian setting, thus exploiting the information contained in the new observations to update the state of knowledge of the model parameters. This approach also helps to reduce the uncertainties that affect the estimate of the residual life expectancy of the structure.

Predicting dam behaviour requires a massive use of complex numerical models including both soil-structure interaction (SSI) [5] and fluid-structure interaction (FSI) [6], whose computational burden is prohibitive without high-performance computing. Therefore, the general polynomial chaos expansion (gPCE) [7] is used to propagate uncertainties through the proposed predictive models of the dam behaviour and to reduce the computational burden by surrogating finite element analysis (FEA) results in the solution of the inverse problem (i.e., definition of gPCE-based predictive models).

In addition, modelling the SSI leads to a large number of numerical modes without experimental correlation, which only act as disruption factors for dynamic SHMs. Sevieri at al. [4] discuss the problem of matching between numerical and experimental modes in the modal analysis of concrete gravity dams and propose an algorithm based on the Markov Chain Monte Carlo (MCMC) method for the selection of numerical modes with experimental correlation. In the present work this algorithm is used to solve the mode matching problem in both the *Training* and *Detection* phases, as discussed in Sect. 4.

The novelty of this study lies in the probabilistic nature and the particular architecture of the proposed framework, which exploits modal information derived from ambient vibrations both to control the structural health state and to reduce the uncertainties in the prediction of the dam behaviour. In fact, the literature review presented in Sect. 2 shows that recent research tends to focus on implementing ambient vibration-based control systems for concrete gravity dams, without proposing a real SHM framework.

Finally the case study proposed in Sect. 5 shows the feasibility of implementing the proposed method for the on-line control of concrete gravity dams.

2 Structural health monitoring systems for concrete gravity dams

SHM is the process of assessing the health state of a structure. The complete definition of a SHM system entails sensor technology, materials technology, numerical modelling and diagnostic techniques [8]. SHM is made up of both hardware components (e.g., instrumentation) and software components (e.g., damage modelling, detection algorithms). Selecting the structural quantity of interest (QI) to be monitored and the definition of damage levels are fundamental steps. They represent the "*structural behaviour*" and its "*threshold*", respectively, the latter is clearly related to a particular damage scenario (DS).

The selected "*structural behaviour*" must be sensitive to damage propagation (i.e., high value of information embedded in the QI) and be easily measurable with a good degree of accuracy. The "*threshold*", which reflects a particular damage scenario, in this context can be defined with respect to a specific limit state (LS) or damage index (DI). The definition of a threshold should also consider the error related to both the measurements and structural health state predictions. Calibrated predictive models of structural behaviour can be successfully used for this purpose [4]. SHM frameworks defined in probabilistic settings and based on calibrated predictive models can detect abnormalities by comparing observations and predictions [9].

SHM systems are composed of the Diagnosis and the Prognosis phases. During the diagnosis, the health state of the structure is assessed locally, at the component level, and globally, in order to detect and locate damaged areas. During the Prognosis, the effects of damage on the structural behaviour are computed, and the residual life expectancy of the construction is thus assessed.

Concrete gravity dams are always equipped with monitoring systems for control purposes, which record environmental measurements, such as the basin level and air and water temperatures. Structural behaviour can be monitored through static or dynamic systems. Static monitoring systems record daily displacements in some reference points of the dam body in both the upstream-downstream and cross-valley directions [10] related to changing environmental conditions. The velocity of this phenomena and the magnitude of the corresponding displacements enable the problem to be addressed as quasi-static.

Dynamic monitoring systems in dam engineering are rarer than static ones and their application is generally limited to research purposes. Due to the large size and mass of the dams, dynamic SHM are generally based on ambient vibrations which are recorded by a network of accelerometers or velocimeters. The data recorded can be directly used to control the health state of the structure or can be processed through OMA techniques [11].

Bukenya et al. [12] reviewed on application of static and dynamic monitoring systems in dam engineering and highlighted that static measurements are commonly used to calibrate predictive models of the structural behaviour in a deterministic setting. On the other hand, only a few applications regard dynamic monitoring systems for dams and no study has presented an SHM framework where calibrated predictive models are actually used for control purposes. Of the various applications that explore the use of ambient vibrations for structural control, some studies present the calibration of dam predictive models in a deterministic setting, but none have proposed a framework for the dynamic SHM of concrete gravity dams.

In addition to the papers mentioned in Bukenya et al. [12], other important research works have been published in recent years. The static SHM systems recently proposed for gravity dams are inspired by the progress made in machine learning. Different architectures have been used to define predictive models of dam static displacements [3, 13–20] in order to improve the accuracy of the prediction and to reduce the computational burden of the classical approaches based on functional approximation [21]. Artificial neural network, support vector machine learning, extreme machine learning, multiple linear regression and general polynomial chaos expansion have been successfully used for the approximation of static dam behaviour.

Another important aspect in the definition of an SHM is the training phase of the predictive model. Most studies are defined in a deterministic setting and regressive methods are used to calibrate dam predictive models. Different approaches have been proposed to improve the performance of predictive models: the hybrid simplex artificial bee colony algorithm (HSABCA) [22], boosted regression trees [23], multilevel-recursive method [17], dynamic time warping (DTW) method, local outlier factor (LOF) [24], chaotic residual errors [19], Random Forest Regression (RFR) [25] and Bayesian inference [3] have been successfully applied in the scientific literature.

Several interesting research works that focus on the definition of static SHM frameworks are described in more detail in the following. Prakash et al. [26] use the principal component analysis for the reduction in the dimension of static predictive models (e.g., displacements, strains). Predictive model coefficients are then calibrated using the least squares method, while the threshold of abnormal behaviour is continuously calibrated through new observations, thus avoiding erroneous warnings. The study of a Bulgarian arch dam shows the feasibility of the proposed procedure.

Su et al. [27] combine the Dempster–Shafer theory of evidence (DST) and Set Pair Theory (SPT), in order to propose a structural health control method for concrete dams, which also supports decision-makers in dam management. This combines multi-source space-time information, such as monitoring systems, and inspections. The study of a hydropower station completed in 1953 proves the efficiency of the method both to control the structural behaviour and to support decision-makers in choosing the best retrofitting intervention.

Hu et al. [28] study the leakages of the Shimantan Reservoir, a concrete dam with penetrating cracks. The authors show that systematic field inspections are fundamental in understanding the cause of the leakages. They also present a predictive model for dam displacements based on a modified version of the Navier-Stokes equations, which is particularly suitable for dams that experience leakages and penetrating cracks.

Lin et al. [20] propose a procedure for the separation of dam displacements into two parts: one relating to the dam behaviour and another relating to the foundation deformation. The idea of partitioned finite element model (FEM) is used to define hybrid equations that enable these two contributions to be separated. Observations recorded by the static monitoring system are used to calibrate the partitioned model, thus estimating the material mechanical parameters. The analysis of a concrete dam is used to verify the validity of the separation method.

Kang et al. [29] propose a static framework for the structural control of concrete dams using long-term air temperature for the simulation of thermal effects. They use the radial basis function network (RBFN) to quantify temperature effects from a long-term air temperature series. The RBFN is then applied instead of the Fourier series, which are commonly adopted for the prediction of thermal effects in dam engineering. The application on a real concrete gravity dam demonstrates the performance of their method.

Dynamic monitoring systems in dam engineering are rarer than static ones. Issues related to SSI and FSI modelling in the dynamic numerical models of concrete dams have hitherto prevented the development of dynamic predictive models and consequently dynamic SHMs [4]. However, there are some studies on the use of ambient vibrations for model calibration purposes.

Cheng et al. [30] propose a SHM approach for concrete dams based on ambient vibrations in which the kernel principle analysis (KPCA) is used to remove the effect of environmental condition variations. Damage is detected by comparing the L_2 norm of the KPCA error calculated during normal conditions with the L_2 norm calculated for the current state of the dam. After detecting the damaged areas, the coordinate modal assurance criterion (COMAC) is used to locate them. The authors do not tackle the mode matching problem and do not define any probabilistic framework.

Hariri-Ardebili et al. [31] study the modal behaviour of an arch dam, highlighting the effect of mechanical parameter uncertainties on the numerical results. The authors present a calibration procedure based on regression to the model parameters, which employs experimental modal characteristics. Again, the procedure is not defined within an SHM framework.

A hierarchical Bayesian method based on ambient vibrations for the dynamic parameter calibration of dam numerical models is proposed by Sevieri et al. [4]. They present a modified version of the Markov Chain Monte Carlo (MCMC) to solve the mode matching problem related to SSI modelling. They use hybrid meta models to surrogate FEA results, thus enabling the Bayesian inference to be applied to dam engineering. The application of the proposed procedure to the case of a real dam demonstrates the validity of this study.

3 Failure mechanisms and damage development in concrete dams

The first step in defining the SHM system is to analyse the damage propagation and failure mechanisms of the structural system. This is carried out in order to select the QIs to be detected and real case histories, numerical models and expert judgements are exploited. Since there are no case histories on concrete dam failures after seismic events [32, 33], numerical models are the only way to predict how such structures deal with collapse [2, 33]. Due to the quasi-brittle nature of the material, collapse mechanisms of concrete dams are mostly driven by tensile crack development [34]. The opening of cracks weakens the structure, thus leading to sliding or rocking.

Crack paths start from both the upstream and the downstream face of the dam and then propagate toward the core [35]. There are four main critical locations where cracks tend to start: (A) the neck area, where there is a change in the downstream face slope; (B) along lift joints at various elevations; (C) along the dam-foundation interface both near to the toe and the dam heel; (D) and at the foundation in near field of the dam. These areas are shown in Fig. 1 adapted from Léger [35].

Three-dimensional models of the dam enable analysts to highlight other failure mechanisms (e.g., those involving vertical contraction joints) which may lead to uncontrolled water release [36] and which cannot be detected through two-dimensional models.

Failure mechanisms of dam cross-sections have been investigated in several studies. Omidi et al. [37] analyse the seismic cracking of concrete gravity dams using a plastic-damage model and assuming different damping approaches. Their results show a high damage concentration in areas A and C in Fig. 1.

Hariri-Ardebili et al. [2] present a state-of-the-art review of seismic fragility analyses of concrete gravity dams. Most studies assume that sliding or rocking only arise in areas A and C in Fig. 1.

In a previous work, De Falco et al. [38] propose an extended version of the “Masonry like” material [39] as a new damage constitutive model for dam concrete. The Koyna dam is studied in terms of both seismic and overflow conditions, and the results are compared with the literature. The study revealed a high concentration of crack paths in areas A and C in Fig. 1.

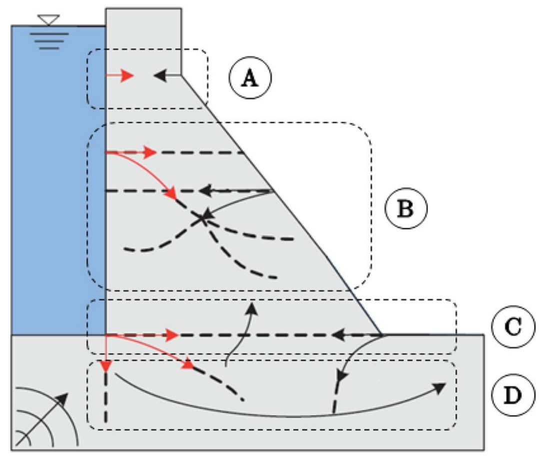

Fig. 1 Crack path critical locations of potential seismic failure modes in the section of concrete dams

Ansari et al. [40] propose a damage index for concrete gravity dams based on crack propagation and sliding safety factors. They demonstrate that this index can be a reliable parameter for the control of the structural health state.

Most studies show that the main failure mechanisms are sliding and rocking due to tensile cracking. A reliable SHM system for concrete gravity dams therefore needs to provide early detection of any variations in a QI with the crack propagation.

4 Proposed SHM framework

4.1 General overview

The present paper proposes a probabilistic SHM framework for concrete gravity dams. Its particular architecture together with the use of gPCE-based predictive models allow for real-time structural control and a better estimation of the remaining life expectancy of the dam. The use of ambient vibrations (Fig. 2) as an information source enables damaged areas to be detected and the dynamic parameters of dam predictive models to be updated within the SHM itself. Epistemic uncertainties related to the mechanical parameters of the materials are thus reduced, and the prediction of the dam behaviour is improved. Both damage detection and SHM are based on a comparison between QIs related to the healthy state of the structure and the current state, i.e., experimental and predicted mode shapes. Since QIs representing structural healthy states vary depending on the environmental conditions, anthropic loads, random factors and

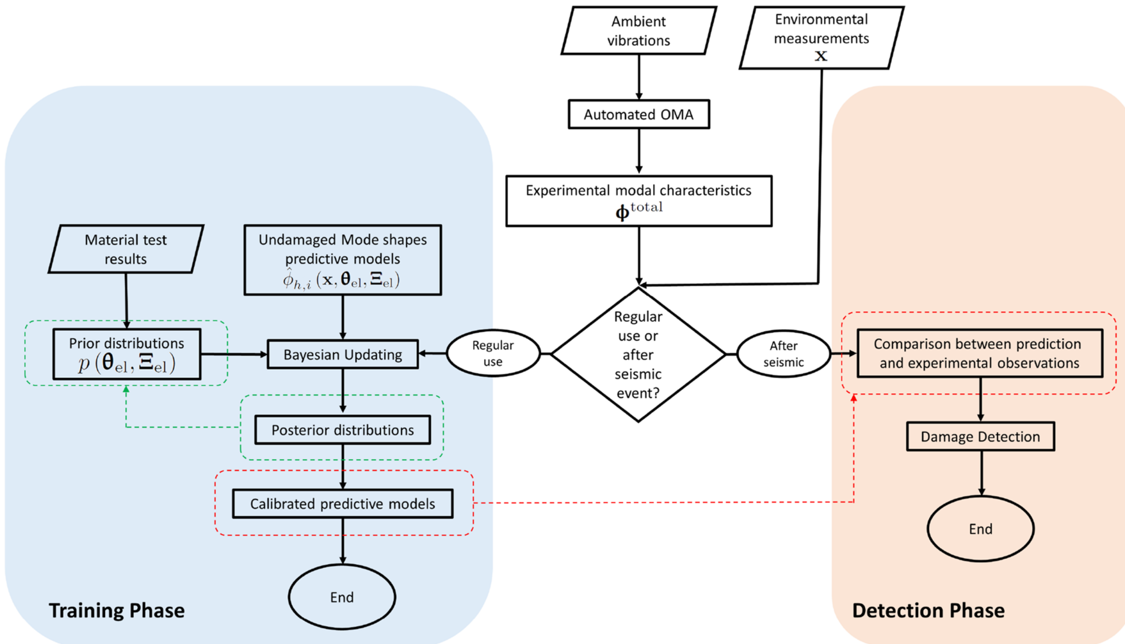

Fig. 2 Flow chart of SHM framework for concrete dams

so on, probabilistic predictive models are needed to forecast their evolution. Predictive models also need to be accurate and fast, to enable the control system to be in real time. In this case, the accuracy of the system is improved by reducing epistemic uncertainties via the Bayesian inference. Using gPCE-based meta models, rather than FE models, leads to more rapid predictions.

The proposed probabilistic framework contributes both to the diagnosis and prognosis steps of the SHM. In fact, the continuous updating of the proposed predictive model reduces the errors, thus refining the predictions themselves and consequently the detection and location of the damage. Likewise, uncertainties are also reduced in the prognosis step, thus improving the estimation of the residual life expectancy of the dam.

The proposed approach has two phases in the hierarchical Bayesian framework [41]: *Training* and *Detection*. During the *Training* phase, predictive models are calibrated using the observations recorded by the monitoring system during the normal operations of the dam. During the *Detection* phase, the structural health state is controlled. The monitoring system records ambient vibrations and environmental measurements, such as basin levels, air humidity rate, water and air temperatures. The structural response to ambient vibrations is analysed through the OMA to determine the system's modal characteristics. In particular, dam mode shapes are used as QI because of their particular sensitivity to damage development.

An additive multivariate probabilistic model [41, 42] is used to statistically describe the relationship among the mechanical parameters of materials, environmental conditions, observed and predicted QIs, and error terms. For the sake of simplicity environmental conditions are collected in $\mathbf{x}$, while the unknown elastic mechanical parameters of materials are collected in $\boldsymbol{\theta}_{el}$. Assuming the system mode shapes as reference QIs, only the elastic parameters of the materials need to be considered as random variables. A parametrization of the problem in terms of the bulk modulus K and shear modulus G [43] reduces the variance of the solution [3]. It is worth noting that the static and dynamic behaviour of dams strictly depend on the environmental conditions [3, 44–49].

The predictive model proposed by Sevieri et al. [4] is used to represent the mode shapes of the system dam-basin-soil. Let us consider q modes of a dam numerical model with m dynamic degrees of freedom ($q \leq m$). By ordering the components of the mode shapes matrix $\boldsymbol{\Phi} = [\boldsymbol{\phi}_1, \dots, \boldsymbol{\phi}_k, \dots, \boldsymbol{\phi}_q]$ in only one vector $\boldsymbol{\phi}^{total}$ with dimension $m \cdot q \times 1$, an index h with $1 \leq h \leq m \cdot q$ can be defined, thus leading to a simplification from a computational point of view [4]. Consequently, the statistical relationship between the ith observation of the hth component of the experimental mode shape $\phi_{h,i}(\mathbf{x}, \boldsymbol{\theta}_{el}, \boldsymbol{\Sigma}_{\phi})$ and the corresponding predicted value $\hat{\phi}_{h,i}(\mathbf{x}, \boldsymbol{\theta}_{el})$ is

$$\phi_{h,i}(\mathbf{x}, \boldsymbol{\theta}_{el}, \boldsymbol{\Sigma}_{\phi}) = \hat{\phi}_{h,i}(\mathbf{x}, \boldsymbol{\theta}_{el}) + \sigma_{\phi_h} \epsilon_{\phi_{h,i}}, \quad h = 1, \dots, m \cdot q \quad i = 1, \dots, l. \tag{1}$$

$\boldsymbol{\Sigma}_{\phi}$ in Eq. 1 is the covariance matrix of the error terms $\sigma_{\phi_h} \epsilon_{\phi_{h,i}}$. In order to improve the prediction capability of the

SHM also the error term is updated, i.e. the components of $\boldsymbol{\Sigma}_{\phi}$. The dimension of the probabilistic problem, and thus the computational burden, strongly increases. Therefore, by assuming that only components that belong to the same mode are correlated, the covariance matrix assumes a block form [4], that is

$$\boldsymbol{\Sigma}_{\phi} =$$

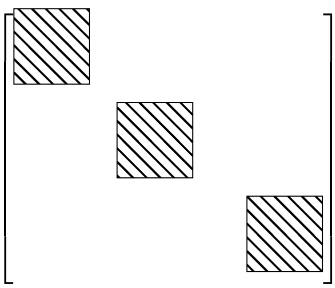

$$. \quad (2)$$

The computational burden can be further reduced by using covariance functions to describe the components of $\boldsymbol{\Sigma}_{\phi}$.

By assuming an exponential form for the covariance function:

$$\mathrm{COV}\left(\phi_r, \phi_s\right) = \frac{1}{\lambda^n} \exp\left[-\left(w_d^n d_{\phi_r,\phi_s}\right)\right], \quad (3)$$

two components ϕ_r and ϕ_s of the same nth mode can be conceived as being correlated through their Euclidean distance d_{ϕ_r,ϕ_s}. The unknown combination coefficients λ^n and w_d^n, which are collected in the vectors $\boldsymbol{\lambda}$ and $\mathbf{w}_d$, respectively, are also updated.

The use of the Bayesian inference within SHM frameworks is particularly effective because of the large amount of recorded data. In the field of engineering modelling, the updating process aims to find the parameter set that leads to the best fit between an observed QI and its prediction obtained with a numerical model [50]. The determination of the parameter values is an inverse ill-posed problem in the Hadamard' sense [51], so a regularisation is needed. The Bayesian inference allows this to be achieved by introducing information about the parameters, namely the prior distributions [52].

As discussed by Sevieri et al. [4], a hierarchical formulation of the updating rule [53] is preferable because it enables the calibration of mean values and standard deviations of parameter distributions. This is fundamental for improving the estimation of the structural fragility during the prognosis phase.

Let us define the vector of the new observations $\mathbf{y}$, which collects the experimental mode shapes obtained by processing the ambient vibrations through OMA, and the vector of the elastic hyper-parameters $\boldsymbol{\Xi}_{\mathrm{el}}$. The prior distribution can thus be written as

$$p\left(\boldsymbol{\theta}_{\mathrm{el}}, \boldsymbol{\Sigma}_{\phi}, \boldsymbol{\Xi}_{\mathrm{el}}\right) = p\left(\boldsymbol{\theta}_{\mathrm{el}}, \boldsymbol{\Sigma}_{\phi} | \boldsymbol{\Xi}_{\mathrm{el}}\right) p\left(\boldsymbol{\Xi}_{\mathrm{el}}\right). \quad (4)$$

By defining the likelihood function $L\left(\mathbf{x}, \boldsymbol{\theta}_{\mathrm{el}}, \boldsymbol{\Sigma}_{\phi}, \boldsymbol{\Xi}_{\mathrm{el}} | \mathbf{y}\right)$ which contains the new observations, the posterior distribution $p\left(\boldsymbol{\theta}_{\mathrm{el}}, \boldsymbol{\Sigma}_{\phi}, \boldsymbol{\Xi}_{\mathrm{el}} | \mathbf{y}\right)$ is obtained through the updating rule

$$\begin{aligned} p\left(\boldsymbol{\theta}_{\mathrm{el}}, \boldsymbol{\Sigma}_{\phi}, \boldsymbol{\Xi}_{\mathrm{el}} | \mathbf{y}\right) &= \kappa L\left(\mathbf{x}, \boldsymbol{\theta}_{\mathrm{el}}, \boldsymbol{\Sigma}_{\phi}, \boldsymbol{\Xi}_{\mathrm{el}} | \mathbf{y}\right) p\left(\boldsymbol{\theta}_{\mathrm{el}}, \boldsymbol{\Sigma}_{\phi}, \boldsymbol{\Xi}_{\mathrm{el}}\right) \\ &= \kappa L\left(\mathbf{x}, \boldsymbol{\theta}_{\mathrm{el}}, \boldsymbol{\Sigma}_{\phi}, \boldsymbol{\Xi}_{\mathrm{el}} | \mathbf{y}\right) p\left(\boldsymbol{\theta}_{\mathrm{el}}, \boldsymbol{\Sigma}_{\phi} | \boldsymbol{\Xi}_{\mathrm{el}}\right) p\left(\boldsymbol{\Xi}_{\mathrm{el}}\right). \end{aligned} \quad (5)$$

Updating procedures based on the Bayesian inference entails defining the prior distribution of the unknown parameters and selecting a computational approach. Calculating the posterior distribution in real problems (i.e., the solution of Eq. 5) is complex [53, 54] because of the integration on manifolds and the large dimension of the problems. The modified version of the numerical algorithm MCMC proposed by Sevieri et al. [4] is herein used to determine the posterior distribution. Given that MCMC is a sampling approach, it requires a large number of analyses, which are computationally expensive. When complex numerical models are used to simulate the structural behaviour, as in the case of concrete dams, the computational cost becomes prohibitive. The use of meta models within the numerical algorithm, rather than exploiting the FEA results, reduces the computational burden [55].

In this study, gPCE-based meta models of the system mode shapes $\hat{\phi}_{h,i}^{\mathrm{gPCE}}\left(\mathbf{x}, \boldsymbol{\theta}^{\mathrm{gPCE}}\left(\boldsymbol{\theta}_{\mathrm{el}}\right)\right)$ surrogate the FEA solutions $\hat{\phi}_{h,i}\left(\mathbf{x}, \boldsymbol{\theta}_{\mathrm{el}}\right)$ (Eq. 6). In order to build the surrogate model, orthogonal basis functions $\boldsymbol{\Psi}_{\alpha}\left(\boldsymbol{\theta}^{\mathrm{gPCE}}\left(\boldsymbol{\theta}_{\mathrm{el}}\right)\right)$ are combined using coefficients collected in $\mathbf{u}^{(\alpha)}(\mathbf{x})$ [7].

$$\begin{aligned} \hat{\phi}_{h,i}\left(\mathbf{x}, \boldsymbol{\theta}_{\mathrm{el}}\right) &\approx \hat{\phi}_{h,i}^{\mathrm{gPCE}}\left(\mathbf{x}, \boldsymbol{\theta}^{\mathrm{gPCE}}\left(\boldsymbol{\theta}_{\mathrm{el}}\right)\right) \\ &= \sum_{\alpha \in \mathbf{I}} \mathbf{u}^{(\alpha)}(\mathbf{x}) \boldsymbol{\Psi}_{\alpha}\left(\boldsymbol{\theta}^{\mathrm{gPCE}}\left(\boldsymbol{\theta}_{\mathrm{el}}\right)\right) \end{aligned} \quad (6)$$

Constructing the response surface also entails defining the gPCE variables $\boldsymbol{\theta}^{\mathrm{gPCE}}\left(\boldsymbol{\theta}_{\mathrm{el}}\right)$ (which are a function of the elastic parameters of the material) and the finite multi-index set $\mathbf{I}$. The combination coefficients $\mathbf{u}^{(\alpha)}(\mathbf{x})$ are determined from the FEA solutions, by applying regression techniques [7] or the Bayesian approach [56]. By exploiting the orthogonality condition of the basis functions, the FEA output statistics (i.e., forward problem solution) can easily be derived through algebraic operations on the combination coefficients [7]. Likewise, a variance-based sensitivity analysis (i.e., Sobol' indices) can easily be conducted by combining the coefficients collected in $\mathbf{u}^{(\alpha)}(\mathbf{x})$ [57], thus quantifying how each random parameter of $\boldsymbol{\theta}_{\mathrm{el}}$ affects the variation of the final result.

Vibration-based damage assessment defined in the Bayesian setting has been used before in the field of SHM [58]. However, in the proposed framework the combination of Bayesian inference, gPCE-based meta models and the modified version of MCMC [4] provides a robust procedure that is applicable to concrete gravity dams.

Each step of the proposed SHM framework is detailed below.

4.2 The training phase

During the *Training* phase, observations recorded by the monitoring system are used to update through the Bayesian Inference the parameters of the predictive model of the mode shapes, which are related to the healthy state of the dam.

Considering l new observations, the likelihood function of Eq. 5 can be written as

$$L\left(\mathbf{x},\boldsymbol{\theta}_{\mathrm{el}},\boldsymbol{\Sigma}_{\phi},\boldsymbol{\Xi}_{\mathrm{el}}\right) \propto \prod_{i=1}^{l} \frac{\exp\left[-\frac{1}{2}\mathbf{r}_i^{\phi^{\mathrm{T}}}\left(\mathbf{x},\boldsymbol{\theta}_{\mathrm{el}},\boldsymbol{\Xi}_{\mathrm{el}}\right)\boldsymbol{\Sigma}_{\phi}^{-1}\mathbf{r}_i^{\phi}\left(\mathbf{x},\boldsymbol{\theta}_{\mathrm{el}},\boldsymbol{\Xi}_{\mathrm{el}}\right)\right]}{\sqrt{\left|2\pi\boldsymbol{\Sigma}_{\phi}\right|}}, \tag{7}$$

where $\mathbf{r}_i^{\phi}\left(\mathbf{x},\boldsymbol{\theta}_{\mathrm{el}},\boldsymbol{\Xi}_{\mathrm{el}}\right) = \left[r_{1,i}^{\phi^{\mathrm{U}}},\ldots,r_{h,i}^{\phi},\ldots,r_{q\cdot m,i}^{\phi}\right]^{\mathrm{T}}$ are the residuals which express the difference between the ith observation of the experimental mode shapes and the related numerical prediction,

$$r_{h,i}^{\phi} = \phi_{h,i}\left(\mathbf{x},\boldsymbol{\theta}_{\mathrm{el}},\boldsymbol{\Sigma}_{\phi,\mathrm{el}}\right) - \hat{\phi}_{h,i}\left(\mathbf{x},\boldsymbol{\theta}_{\mathrm{el}},\boldsymbol{\Xi}_{\mathrm{el}}\right). \tag{8}$$

The prior distributions of the material elastic parameters (Eq. 5) can be derived from the material test results, which are usually available for existing concrete dams. On the other hand, non-informative prior distributions can be used for parameters whit no physical meaning, such as $\boldsymbol{\lambda}$ and $\mathbf{w}_d$ [41].

4.3 The detection phase

The *Detection* phase detects damage by comparing experimental mode shapes, currently observed by processing ambient vibrations with OMA, with those of the healthy dam simulated by the calibrated predictive model. The computational speed achieved through the surrogate model allows for the real-time structural control in this step.

Three fundamental aspects must be considered in the definition of the *Detection* phase: selection of the OMA technique, selection of the control frequency, and the definition of thresholds that reflect structural abnormal behaviours.

Signal processing and selection of the most appropriate OMA technique are fundamental steps for the accurate estimation of experimental mode shapes and frequencies. Even tough this topic is outside the scope of the present study, it can be stated that automated OMA techniques [11] are certainly appropriate for the installation of a continuous SHM system.

The control frequency is the time period between two subsequent controls of the health state of the structure. This important aspect is usually related to the computational power available and the storage capacity. The gPCE-based models adopted in this study considerably reduce the computational burden, thus the computational power required is no longer a problem. On the other hand, continuous control systems require more storage capacities than those related to event-triggered systems. Continuous SHMs with relatively high control frequency thus require more storage capacity than daily ones. Clearly the choice of the best control frequency cannot be generalised and it must be accurately evaluated by balancing available storage capacity and required structural safety.

Defining a suitable threshold related to a particular damage state involves the physical phenomenon and the accuracy of the observations and predictions. Regarding this latter, the proposed approach allows analysts to estimate the trust level in the discrepancy between recorded and predicted QI by updating the covariance matrix $\boldsymbol{\Sigma}_{\phi}$ of the error terms. A probabilistic study of the physical phenomenon is required in order to correlate a variation in the monitored QI with a particular damage scenario. In fact, if there are no case studies, only numerical models can help to investigate how concrete dams react during a collapse. Due to the many uncertainties involved in this calculation, such a study should be conducted within a robust probabilistic framework. Since each concrete gravity dam is characterised by its own construction features and geometric characteristics, scenario analyses for the determination of suitable thresholds should be performed for every individual dam.

5 Case of study

5.1 Dam description

The proposed SHM framework is applied to a large concrete dam in Italy for which material test results and ambient vibration records are available. Since the observations were recorded during the normal use of the dam, they are related to a healthy state of the structure in this study. However, given that there are no information on how the dam would behave when damage occurs, a high-fidelity model is used to simulate such conditions.

The dam is situated in a high seismic area in Italy. It is 55 m tall and 199.20 m in length, with no vertical contraction joints. The near-field of the dam is made up of two different types of soil: an arenaceous mass and a marl mass.

As outlined in Sect. 4, the elastic parameters of the materials (i.e., the bulk moduli K and the shear moduli G) are treated as random variables. The concrete parameters are indicated with the subscript C, while those of the arenaceous soil and those of the marl mass are indicated with A and M subscripts, respectively.

Therefore, in this study the elastic model parameters are collected in $\boldsymbol{\theta}_{\rm el} = \left[K_C, G_C, K_A, G_A, K_M, G_M\right]^{\rm T}$. In addition, assuming that they are log-normally distributed with mean values collected in $\boldsymbol{\xi}^{\mu}_{\rm el} = \left[\xi^{\mu}_{K_C}, \xi^{\mu}_{G_C}, \xi^{\mu}_{K_A}, \xi^{\mu}_{G_A}, \xi^{\mu}_{K_M}, \xi^{\mu}_{G_M}\right]^{\rm T}$ and variances collected in $\boldsymbol{\xi}^{\sigma}_{\rm el} = \left[\xi^{\sigma}_{K_C}, \xi^{\sigma}_{G_C}, \xi^{\sigma}_{K_A}, \xi^{\sigma}_{G_A}, \xi^{\sigma}_{K_M}, \xi^{\sigma}_{G_M}\right]^{\rm T}$, their hyper-parameter vector becomes $\boldsymbol{\Xi}_{\rm el} = \left[\boldsymbol{\xi}^{\mu}_{\rm el}, \boldsymbol{\xi}^{\sigma}_{\rm el}\right]^{\rm T}$.

Only the basin level variation is considered as a measurable variable $\mathbf{x}$ in this application, because no information on temperatures and humidity was available. Moreover, the results of only one ambient vibration experimental campaign are available. The temperatures and humidity can thus be assumed to be constant during the test, and consequently their effects on the dam behaviour can be neglected.

5.2 Dynamic experimental campaign

The *Training* phase is performed by using the information acquired from the Italian Civil Protection in 2016 during an experimental campaign. The aim of the survey was the modal identification of the system using its modal characteristics obtained by processing ambient vibrations using OMA techniques. Fifteen high performance 1 Hz Seismometer LE-3Dlite (Lennartz Electronic GmbH), placed in the upper part of the structure, were used to record ambient vibrations. Two-hour recordings with a sampling frequency of $f_s = 200$ Hz were performed. The data and results are presented in the experimental campaign report [59] which is available on-line [60]. In particular, the first three modes were identified (Fig. 3) by applying the Enhanced Frequency Domain Decomposition (EFDD) method with a basin level equal to 856.2 m.a.s.l., i.e. 40.8 m from the bottom of the dam.

5.3 Material test results and prior distributions

Several different experimental campaigns were carried out over time to investigate the quality of the concrete and soil. The results of the 2012 experimental campaign (Table 1) are used in this work for the definition of the hyper-prior distributions. The hyper-prior distributions of the mechanical characteristics of the material are assumed log-normal: those of the hyper-parameters $\boldsymbol{\xi}^{\mu}_{\rm el}$ are directly derived from the material test results, while those of the hyper-parameters $\boldsymbol{\xi}^{\sigma}_{\rm el}$ have mean values equal to the standard deviations obtained during experimental tests and coefficient of variations (CoVs) equal to 10%. The assumed values of CoVs avoid numerical problems in the algorithm for the inverse problem solution, therefore, in the absence of any information on them, it seems to be a reasonable choice. In addition, only $\boldsymbol{\xi}^{\mu}_{\rm el}$ are updated in the proposed procedure, then every reasonable choice on $\boldsymbol{\xi}^{\sigma}_{\rm el}$ does not affect the final result. The hyper-prior distributions of the mechanical parameters are reported in Table 2. The prior distributions of the parameters with no physical meaning, such as those of the covariance function, are modelled as non-informative.

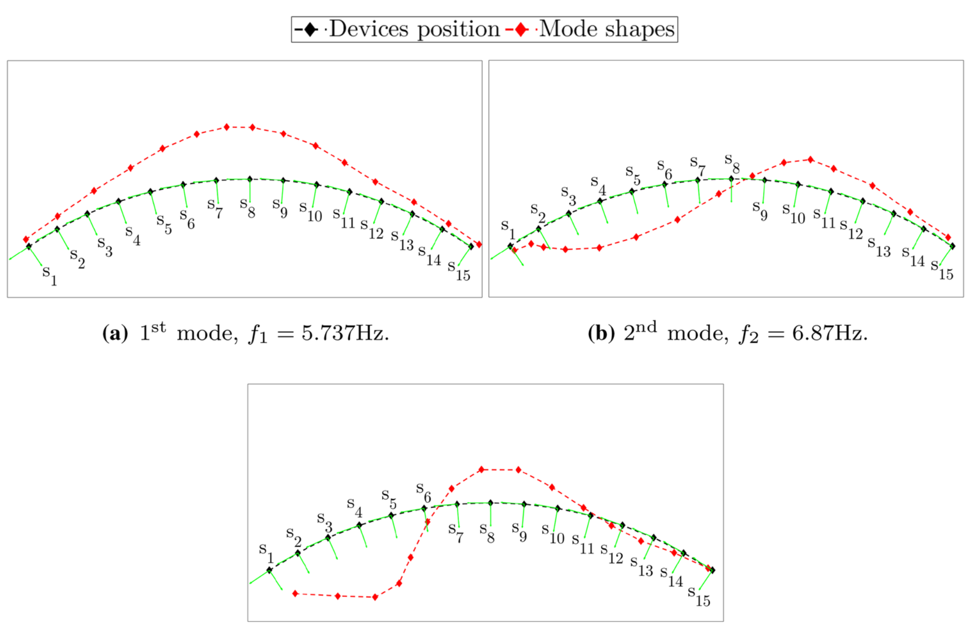

(a) 1st mode, $f_1 = 5.737$Hz. (b) 2nd mode, $f_2 = 6.87$Hz. (c) 3rd mode, $f_3 = 8.896$Hz.

Fig. 3 Experimental mode shapes

5.4 Construction of the FE model and gPCE surrogate model

The predictive models $\hat{\phi}_{h,i}(\mathbf{x}, \boldsymbol{\theta}_{\mathrm{el}}, \boldsymbol{\Xi}_{\mathrm{el}})$ of the mode shapes of the dam (Sect. 4) are based on the gPCE, which is trained on the solution of the modal analysis of a FE model.

Starting from the topographic maps and the original technical drawings of the dam, the system dam-basin-soil model is constructed in a CAD program. The final geometry is then imported into ABAQUS 6.14 [61], the software used for the FEAs. The SSI is considered by modelling the near-field with as an elastic medium and using infinite elements [5] to reproduce the unboundedness of the soil domain. Acoustic elements are used to model the basin and its interaction with the dam body and the soil domain as well. Low reflecting boundary conditions [6] are used at the edges of the fluid domain to avoid the reflection of seismic waves.

The FE model is composed of 13,280 quadratic tetrahedral mechanical elements (C3D10) for the dam body and the foundation soil, and 237 linear hexahedral infinite elements (CIN3D8) for the soil boundary conditions. The number of the 4-node linear tetrahedron fluid elements (AC3D4) of the reservoir depends on the water level that is a measurable variable. Materials are assumed linear elastic, since the calculation of gPCE combination coefficients is based on the modal analysis.

Once the FE model is created, the gPCE must defined. Hermitian polynomials are used for the definition of the orthogonal basis functions, and the combination coefficients of the polynomial expansion (Sect. 4) are determined on the FEA outputs. The parameters sets of theses FEAs are randomly sampled from the prior distributions of the mechanical parameters, while the basin levels $\mathbf{x}$ is deterministically discretised. The prior distributions used to for this task are assumed log-normally distributed with parameters derived from the mean values of $\boldsymbol{\xi}_{\mathrm{el}}^{\mu}$ and $\boldsymbol{\xi}_{\mathrm{el}}^{\sigma}$ (Table 2). The basin level varies from the bottom of the dam to the maximum level (55 m), with steps of 10 m, and, in order to improve the accuracy of the solution, also basin levels equal to 40.8 m (basin level during the experimental campaign) 55 m (maximum level) are considered. The discretization of the measurable variables depends on the aims of the study, then such a coarse discretization is acceptable only to show the feasibility of the method, while a much more refined discretization is well recommended for the implementation of a dynamic SHM. A total of 150 numerical analyses, characterised by different parameters sets randomly sampled from the prior distributions, are finally performed for each basin level. The FEA results are then used for the calibration of the gPCE coefficients by applying the procedure proposed by Rosić et al. [56]. A sensitivity analysis is performed to select the degree of the polynomial expansion, which minimise the gPCE error. After 200 new analyses, performed by randomly sampling from the previously defined prior distributions and from the set of the measurable variables, the mean values of the gPCE error are calculated for the first 17 frequencies of the system (Fig. 4) considering 3th, 4th and 5th polynomial orders. The error is herein defined as the difference between the FEA result and the related gPCE prediction divided by the FEA result itself. The sensitivity analysis shows that the 5th order polynomial expansion provides the smallest error both in terms of frequencies and mode shapes.

Table 1 Material test results

	E_C (MPa)	ν_C	ρ_C (kg/m^3)	$f_{t,C}$ (MPa)	$f_{c,C}$ (MPa)	E_A (MPa)	ν_A	ρ_A (kg/m^3)	E_M (MPa)	ν_M	ρ_M (kg/m^3)
Mean	34620	0.16	2270	2	16.7	21000	0.16	1800	7000	0.22	1800
SD	12498	0.06	189.17	1.1	5.16	9545	0.07	–	3181.8	0.1	–

Table 2 Hyper-prior distributions of the mechanical parameters

	ξ^{μ}_{m,K_C} (MPa)	ξ^{μ}_{m,G_C} (MPa)	ξ^{μ}_{m,K_A} (MPa)	ξ^{μ}_{m,G_A} (MPa)	ξ^{μ}_{m,K_M} (MPa)	ξ^{μ}_{m,G_M} (MPa)
Distr.	Log-normal	Log-normal	Log-normal	Log-normal	Log-normal	Log-normal
Mean	16971	14922	10294	9051.7	4166.7	2868.9
SD	6109.6	5372.1	4411.8	3879.3	1785.7	1229.5
	ξ^{σ}_{m,K_C} (MPa)	ξ^{σ}_{m,G_C} (MPa)	ξ^{σ}_{m,K_A} (MPa)	ξ^{σ}_{m,G_A} (MPa)	ξ^{σ}_{m,K_M} (MPa)	ξ^{σ}_{m,G_M} (MPa)
Distr.	Log-normal	Log-normal	Log-normal	Log-normal	Log-normal	Log-normal
Mean	6109.6	5372.1	4411.8	3879.3	1785.7	1229.5
SD	611.0	537.2	441.2	387.9	178.6	123.0

5.5 The high-fidelity FE model

The damaged behaviour of the dam is simulated through a high-fidelity model having the same geometry of the one described in Sect. 5.4, but with a much more refined mesh and a non-linear constitutive model for the concrete. The mesh is composed of 15,936 quadratic tetrahedral mechanical elements (C3D10) for the dam body and the soil domain, and 6873 linear tetrahedral acoustic elements (AC3D4) for the basin. Moreover, 474 linear hexahedral infinite elements (CIN3D8) are used to model the unboundedness of the soil domain, while low reflecting boundary conditions are applied at the edges of the basin. The minimum mesh size is one tenth of the smallest wavelength of the seismic motion used in the seismic analysis described in the next sections.

As the high-fidelity model is deterministic, the basin level is at the maximum height, i.e. 55.5 m, thus considering the worst case scenario for the seismic analysis.

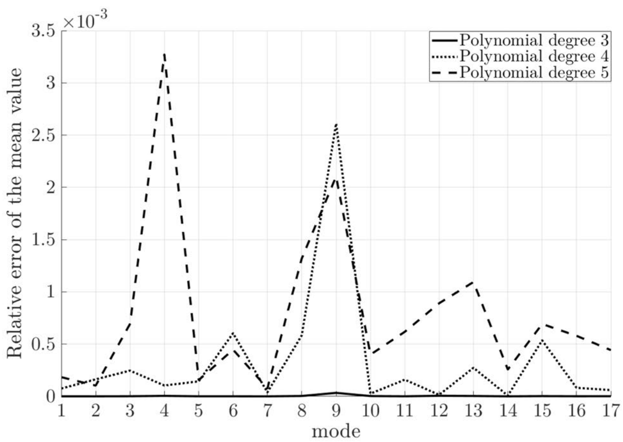

(a) Error of the mean value.

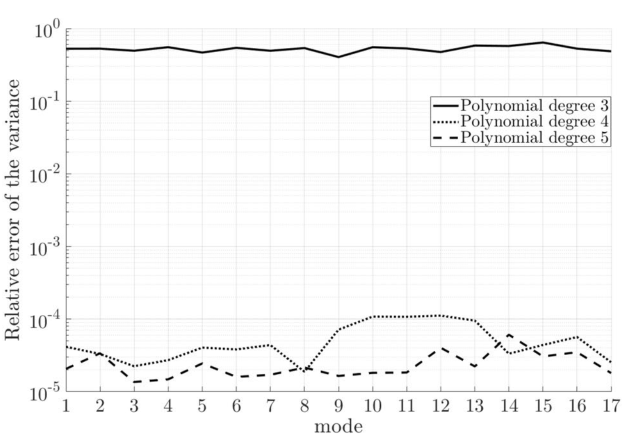

(b) Error of the standard deviation.

Fig. 4 Relative errors of the mode shapes meta model of the Scandarello dam

By assuming that the failure can occur only in the dam body due to tensile crack propagation, an elastic-plastic damage model (the concrete damage plasticity model) [62] is adopted for the dam concrete, while the soil is assumed linear-elastic. The parameters of the damage law and those of the plastic flow can be found in the scientific literature [37] and they are reported in Table 3. More specifically, ψ is the dilation angle, ε is is the eccentricity that defines the rate at which the flow potential approaches the asymptote, σ_{b0}/σ_{c0} is the ratio of initial equibiaxial compressive yield stress to initial uniaxial compressive yield stress and K_c is the ratio of the second stress invariant on the tensile meridian to that on the compressive meridian. In this study, the tensile strength is fixed equal to 1.45 MPa, while the fracture energy is assumed equal to 150 N/m.

5.6 Training phase

In the *Training* phase, the experimental mode shapes described in Sect. 5.2 are used to calibrate the gPCE-based predictive models defined in Sect. 5.4. This fundamental step aims to reduce the uncertainties involved in the prediction of the dam behaviour and to estimate its error as well. In a real control system, the procedure described in this Section, which is applied only to a single observation, is repeated every time new data are available.

The predictive model parameters are updated by following the procedure described in Sect. 4.2. The procedure proposed by Sevieri et al. [4] is used to solve the inverse problem. This numerical algorithm, based on MCMC, requires setting up few parameters: the initial mechanical parameter set, the number of steps and the proposal distributions. The mean values of the hyper-prior distributions of $\boldsymbol{\xi}_{el}^{\mu}$ are used to define the initial mechanical parameter set. Normal distributions with mean values equal to zero and standard deviations equal to 10% of the prior distribution ones are used as proposal distributions. The convergence of the algorithm, checked through the probabilistic metric proposed by Brooks et al. [63], is achieved in 10,000 steps (1000 burn-in).

Fig. 5 shows the comparison between prior and posterior distributions of K and G, while the posterior statistics are reported in Table 4. The posterior distributions reported in Fig. 5 are used for the definition of the gPCE (Sect. 5.4). The comparison between experimental and numerical frequencies shown in Table 5 confirms the good agreement between them. The good agreement between experimental and predicted mode shapes can be observed in terms of modal assurance criterion (MAC) [11]. Each MAC matrix

Table 3 Plastic flow parameters

ψ (°)	ε	σ_{b0}/σ_{c0}	K_c
36.31	0.1	1.16	0.66

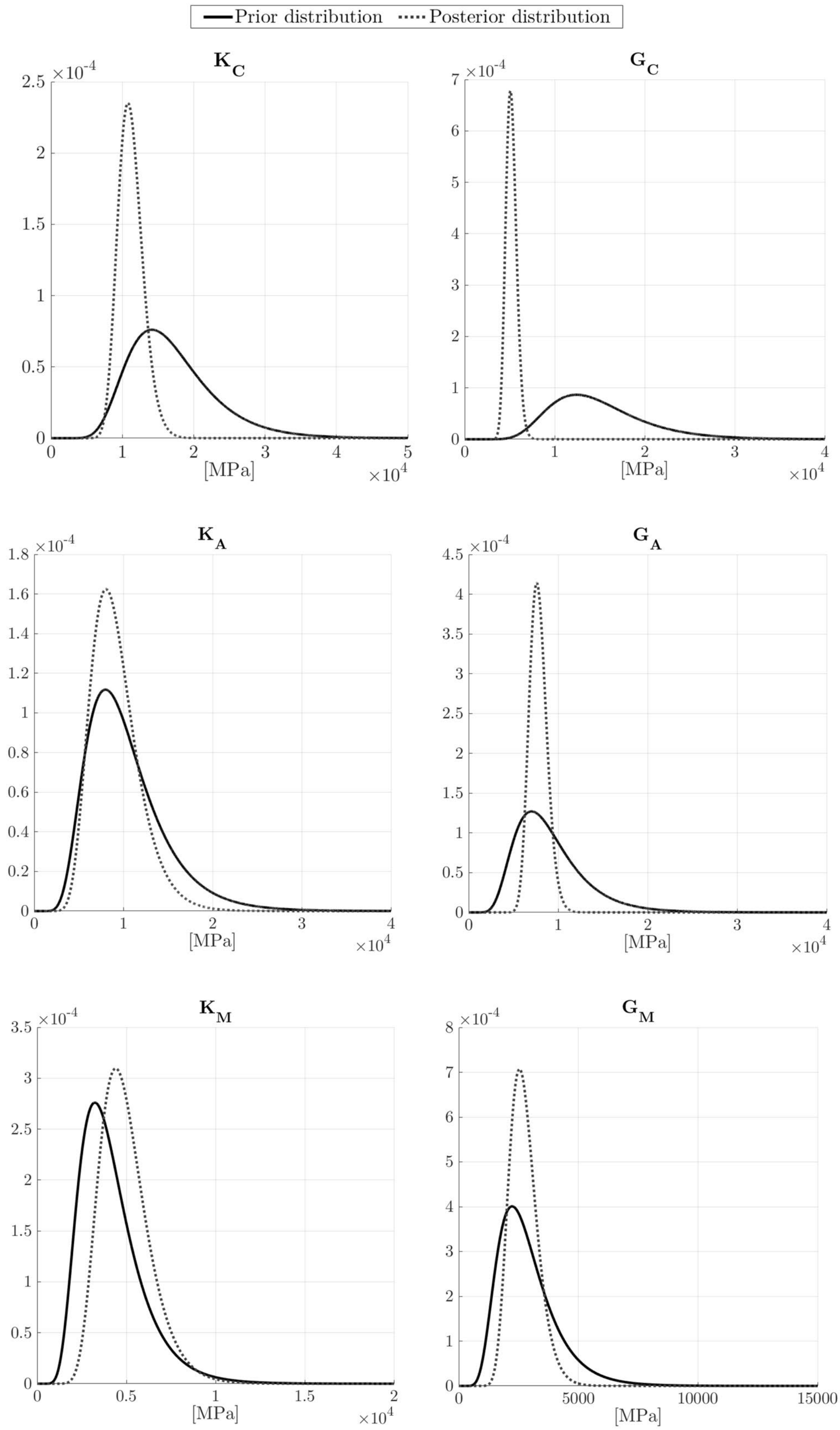

Fig. 5 Comparison between prior and posterior distributions of K and G

element represents the correlation between an experimental mode and its prediction. MAC values close to 1 indicate a high correlation between the two modes. Figure 6 shows that only three modes have a sufficiently high correlation, while most numerical modes have low correlation with the experimental ones.

The inverse analysis algorithm adopted in this work automatically selects the correlated modes, thus solving the previously discussed mode matching problem.

5.7 Detection phase

During the *Detection* phase, the observed experimental mode shapes are compared to those obtained from the gPCE-based predictive models. In this application, the comparison is the point-to-point difference between experimental and predicted mode shapes. As discussed in the Sect. 4.3 the comparison criteria, as well as the definition of the thresholds, depends on case study and the available information. In the absence of real records providing the modal characteristics of the damaged dam, the high-fidelity FE model described in Sect. 5.5) is used to simulate the experimental mode shapes related to three different damage scenarios.

The three DSs considered in this study are defined with regard to the development of tensile crack paths. Only crack paths with tensile damage variable of the concrete damage plasticity model d_t higher than 0.3 are considered. DS1 is thus achieved when cracks appear in one of the critical areas of Fig. 1 (localised damage), DL2 is achieved when crack paths grow toward the core of the dam (diffuse damage), and DL3 is achieved when widespread damage or crossing crack path appear.

The reference seismic event for the construction of the DSs is the magnitude 6.2 earthquake occurred on 24 August 2016 at 01:36 UTC in Central Italy. The first period spectral acceleration $S_a(T_1)$ is used herein as reference intensity measure of the ground motion. The seismic input recorded by the Amatrice station, characterised by $S_a(T_1)$ equal to 1.5622 g, is considered and scaled to the attainment of the three defined DSs. The scaled action is applied as boundary condition at the base of the near-field after a deconvolution step [64].

DS1 is achieved for $S_a(T_1) = 0.2107\,g$, DS2 is achieved for $S_a(T_1) = 0.4328g$ and DS3 is achieved for $S_a(T_1) = 0.472g$. The three preselected DSs can be achieved only by reducing the original seismic input. The tensile strength, assumed equal to 1.45 MPa, is a conservative value if compared to the material test results, this fact justifies the results of the seismic analyses.

The DSs are reported in Fig. 7. Following the procedure discussed in Sect. 4.3, structural damage is detected by comparing the experimental mode shapes related to different DSs (obtained in this study from the high-fidelity mode) with the corresponding predictions (derived from the calibrated gPCE-based predictive models). Figure 8 shows the comparison between observations and predictions. The devices layout is the same adopted during the experimental campaign described in Sect. 5.2.

The results highlight that an abnormal behaviour of the system can be easily detected from the first three principal modes of the dam for DS2 and DS3 (Fig. 8). In both these cases, observed and predicted mode shapes show large differences. Whereas, for DS1 predictions and observations are relatively close, even if their difference is higher than the error of the prediction itself. The damage detection in case of DS1 is of primary importance for the structural control. Figure 9 shows the histogram of the discrepancy between predictions and observations for each device in case of DS1. The discrepancy is herein defined as the percentage variation of the prediction plus its standard deviation. Clearly the higher modes better indicate abnormal behaviour, even tough the maximum discrepancy reaches 1% in the middle of the dam crest. The monitoring system, including hardware and software components, should be designed in order to achieve this accuracy.

6 Concluding remarks

Concrete gravity dams are fundamental infrastructure for the sustainability of a country. Most of them were designed/built without concerns for their dynamic behaviour, therefore

Table 4 Posterior distributions of the elastic parameters

	ξ^{μ}_{m,K_C} (MPa)	ξ^{μ}_{m,G_C} (MPa)	ξ^{μ}_{m,K_A} (MPa)	ξ^{μ}_{m,G_A} (MPa)	ξ^{μ}_{m,K_M} (MPa)	ξ^{μ}_{m,G_M} (MPa)	ξ^{σ}_{m,K_C} (MPa)	ξ^{σ}_{m,G_C} (MPa)	ξ^{σ}_{m,K_A} (MPa)
Mean	11184.2	5186.5	9156.3	7789.7	4958.1	2724.6	1749.1	598.31	2732.74
SD	559.22	378.61	631.78	545.28	242.94	168.93	155.66	45.77	240.42
	ξ^{σ}_{m,G_A} (MPa)	ξ^{σ}_{m,K_M} (MPa)	ξ^{σ}_{m,G_M} (MPa)	λ^1	λ^2	λ^3	w_d^1	w_d^2	w_d^3
Mean	982.26	1422.50	598.3	25.16	39.09	34.28	0.0074	0.0261	0.0053
SD	68.03	137.29	45.01	5.24	6.25	2.92	0.0096	0.1615	0.0132

Table 5 Comparison between experimental and numerical frequencies

	Experimental frequencies	Numerical Frequencies
f_1 (Hz)	5.737	5.592
f_2 (Hz)	6.870	6.691
f_3 (Hz)	8.896	9.183

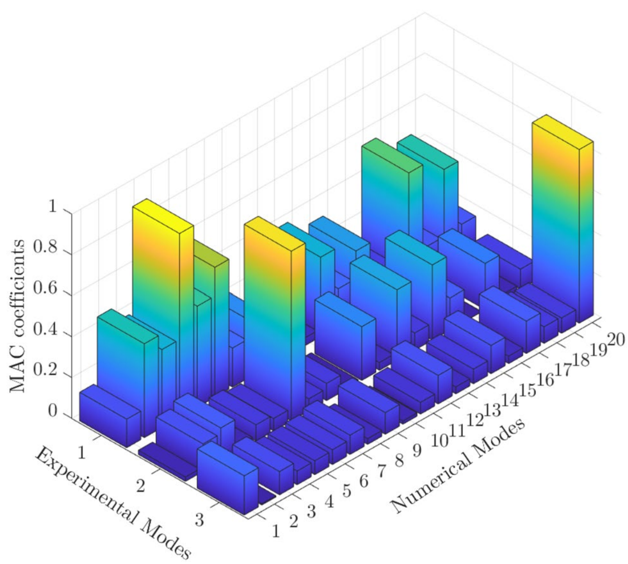

Fig. 6 MAC matrix between experimental frequencies and numerical ones calculated using the mode shapes predictive model

do not meet the seismic reliability levels required by our society.

Dynamic structural health monitoring (SHM) systems play a fundamental role both in terms of controlling concrete dams and in terms of reducing the uncertainties involved in the seismic assessment of such structures. Exploiting ambient vibrations as source of information is an interesting option in dam engineering. In fact, in this strategy continuous monitoring systems can be installed without requiring any additional device for the excitation of the dam, thus reducing the overall cost. However, only few applications of ambient vibration-based monitoring systems to concrete gravity dams are available in the scientific literature. None of them propose probabilistic frameworks.

A new probabilistic framework for ambient vibration-based SHM for concrete dams is proposed in this paper. With the proposed SHM, the structural health state of the dam can be controlled and the mechanical parameters of the numerical model can be updated. The uncertainties involved in the predictive models of the dam are reduced, thus improving the structural control itself and the estimation of the remaining life expectancy of the structure. The particular SHM architecture is made up of two different steps defined in the Bayesian setting: the *Training* phase and the *Detection* phase. During the *Training* phase, ambient vibrations are first processed through Operational Modal Analysis (OMA) methods to determine the modal characteristics of the system. These characteristics are then used to calibrate predictive models of the structural behaviour based on the general Polynomial Chaos Expansion (gPCE). The use of the gPCE

Fig. 7 Damage scenarios, *Detection* phase

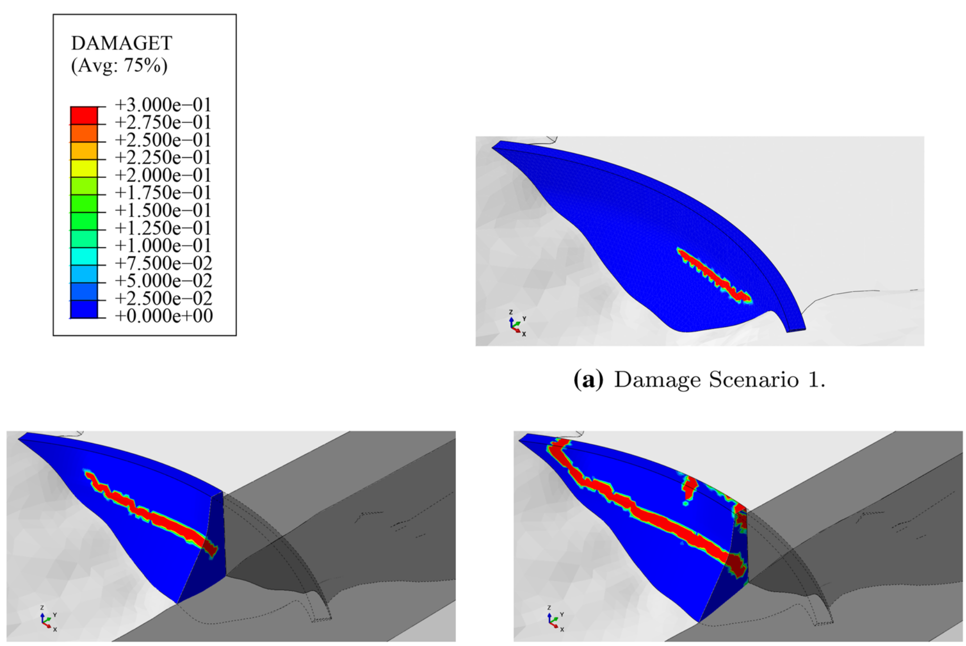

(a) Damage Scenario 1.

(b) Damage Scenario 2.

(c) Damage Scenario 3.

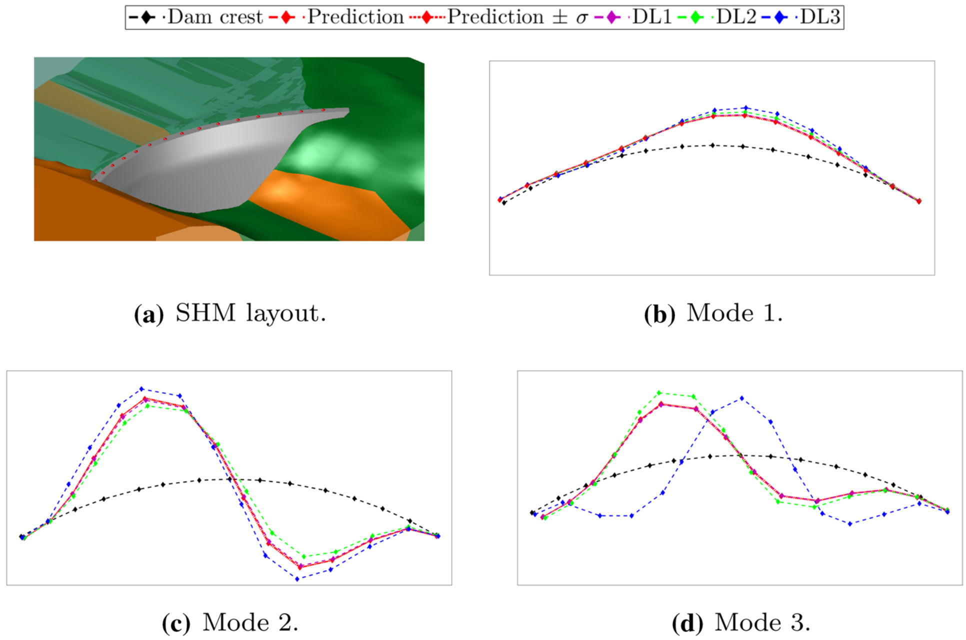

Fig. 8 Comparison between experimental mode shapes and predictions, *Detection* phase

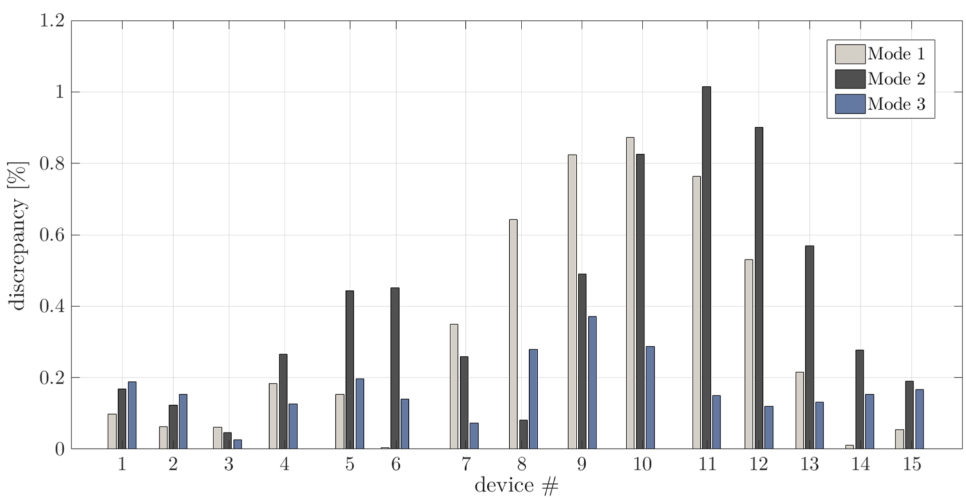

Fig. 9 Discrepancy between predictions and experimental mode shapes for each device (DL1)

for surrogating numerical models of the dam means that the procedure can be defined in the Hierarchical Bayesian framework without high-performance computing. In addition, the definition of the framework in the Bayesian setting reduces the uncertainties involved in the predictive models themselves.

The calibrated predictive models are then used in the *Detection* phase in order to assess damaged areas. This phase is based on comparing predictions with current experimental observations. The computational speed and accuracy achieved with the use of gPCE-based predictive models enables the proposed dynamic SHM to be used for real-time control of the structures. Another important aspect in this fundamental step is the definition of a threshold for the detection of abnormal behaviour in the dam. However, this topic is not among the aims of the present paper, which is more focused on the definition of the SHM framework.

We applied the proposed framework to a real large concrete dam located in a high-seismic area in Italy, for which real ambient vibration records and material test results are available. The case study shows the feasibility of our approach in real cases and has important implications. The use of gPCE-based meta models is fundamental for the implementation of the real time control, and the inverse analysis algorithm used for the solution of the Bayesian problem allows the mode matching problem to be solved, which is a crucial issue in dam engineering. The idea of defining a threshold with regard to different Damage Scenarios (DSs) is an interesting idea which allows intervention strategies to be set up. The accuracy of the

SHM system should be increased as much as possible by optimising the device layout (i.e., decrease the required accuracy level for detecting a particular DS) or by using a more sensitive quantity of interest (such as the derivatives of mode shapes). We plan to investigate these topics in future works.

References

1. ASDSO (2011) State and federal oversight of dam safety must be improved. Magazine of Association of State Dam Safety Officials (ASDSO)
2. Hariri-Ardebili MA, Saouma VE (2016) Seismic fragility analysis of concrete dams: a state-of-the-art review. Eng Struct 128(October):374–399
3. Sevieri G, Andreini M, De Falco A, Matthies HG (2019) Concrete gravity dams model parameters updating using static measurements. Eng Struct 196:109231
4. Sevieri G (2019) The seismic assessment of existing concrete gravity dams: FE model uncertainty quantification and reduction. Ph.D. thesis, University of Pisa/Technical University of Braunschweig
5. De Falco A, Mori M, Sevieri G (2018) Simplified soil-structure interaction models for concrete gravity dams. In: Proceedings of the 6th European conference on computational mechanics, 7th European conference on computational fluid dynamics. Glasgow, pp 2269–2280
6. De Falco A, Mori M, Sevieri G (2018) FE models for the evaluation of hydrodynamic pressure on concrete gravity dams during earthquakes. In: Proceedings of 6th European conference on computational mechanics, 7th European conference on computational fluid dynamics. Glasgow, pp 1731–1742
7. Xiu D (2010) Numerical methods for stochastic computations. Princeton University Press, Princeton
8. Gopalakrishnan S, Ruzzene M, Hanagud S (2011) Computational techniques for structural health monitoring, 1st edn. Springer, Berlin
9. Chatzi EN (2016) Identification methods for structural health monitoring, vol 567, 1st edn. Springer, Berlin
10. ICOLD (2000) Bullettin 118: automated dam monitoring systems guidelines and case histories. Technical report, ICOLD, Paris
11. Brincker R, Ventura CE (2015) Introduction to operational modal analysis. Wiley, Hoboken
12. Bukenya P, Moyo P, Beushausen H, Oosthuizen C (2014) Health monitoring of concrete dams: a literature review. J Civ Struct Health Monit 4:235–244
13. Kao C-Y, Loh C-H (2013) Monitoring of long-term static deformation data of Fei-Tsui arch dam using artificial neural network-based approaches. Struct Control Health Monit 20:282–303
14. Mata J, Tavares de Castro A, Sá da Costa J (2014) Constructing statistical models for arch dam deformation. Struct Control Health Monit 21:423–437
15. Su H, Chen Z, Wen Z (2016) Performance improvement method of support vector machine-based model monitoring dam safety. Struct Control Health Monit 23:252–266
16. Kang F, Liu J, Li J, Li S (2017) Concrete dam deformation prediction model for health based on extreme learning machine. Struct Control Health Monit 24:e1997
17. Wei B, Gu M, Li H, Xiong W, Xu Z (2018) Modeling method for predicting seepage of RCC dams considering time-varying and lag effect. Struct Control Health Monit 25:e2081
18. Shao C, Gu C, Yang M, Xu Y, Su H (2018) A novel model of dam displacement based on panel data. Struct Control Health Monit 25:e2037
19. Wei B, Yuan D, Xu Z, Li L (2018) Modified hybrid forecast model considering chaotic residual errors for dam deformation. Struct Control Health Monit 25:e2188
20. Lin C, Li T, Liu X, Zhao L, Chen S, Qi H (2019) A deformation separation method for gravity dam body and foundation based on the observed displacements. Struct Control Health Monit 26:e2304
21. Andreini M, De Falco A, Marmo G, Mori M, Sevieri G (2017) Modelling issues in the structural analysis of existing concrete gravity dams. In: Proceedings of the 85th ICOLD annual meeting. Prague, pp 363–383
22. Kang F, Li J, Xu Q (2009) Structural inverse analysis by hybrid simplex artificial bee colony algorithms. Comput Struct 87:861–870
23. Salazar F, Toledo MÁ, González JM, Onate E (2017) Early detection of anomalies in dam performance: a methodology based on boosted regression trees. Struct Control Health Monit 24:e2012
24. Hu J, Ma F, Wu S (2018) Anomaly identification of foundation uplift pressures of gravity dams based on DTW and LOF. Struct Control Health Monit 25:e2153
25. Dai B, Gu C, Zhao E, Qin X (2018) Statistical model optimized random forest regression model for concrete dam deformation monitoring. Struct Control Health Monit 25:e2170
26. Prakash G, Sadhu A, Narasimhan S, Brehe JM (2018) Initial service life data towards structural health monitoring of a concrete arch dam. Struct Control Health Monit 25:e2036
27. Su H, Wen Z, Sun X, Yan X (2018) Multisource information fusion-based approach diagnosing structural behavior of dam engineering. Struct Control Health Monit 25:e2073
28. Hu J, Ma F, Wu S (2018) Comprehensive investigation of leakage problems for concrete gravity dams with penetrating cracks based on detection and monitoring data: a case study. Struct Control Health Monit 25:e2127
29. Kang F, Li J, Zhao S, Wang Y (2019) Structural health monitoring of concrete dams using long-term air temperature for thermal effect simulation. Eng Struct 180:642–653
30. Cheng L, Yang J, Zheng D, Li B, Ren J (2015) The health monitoring method of concrete dams based on ambient vibration testing and kernel principle analysis. Schock Vib
31. Hariri-Ardebili MA, Mahdi Seyed-Kolbadi S, Saouma VE, Salamon JW, Nuss LK (2019) Anatomy of the vibration characteristics in old arch dams by random field theory. Eng Struct 179:460–475
32. Hall JF (1988) The dynamic and earthquake behaviour of concrete dams: review of experimental behaviour and observational evidence. Soil Dyn Earthq Eng 7(2):58–121
33. Zhang L, Peng M, Chang D, Xu Y (2015) Dam failure mechanisms and risk assessment. Wiley, Singapore

34. Weerheijm J (2013) Understanding the tensile properties of concrete. Woodhead Publishing, Sawston
35. Léger P (2007) Reducing the earthquake induced damage and risk in monumental structures: experience at Ecole Polytechnique de Montreal for large concrete dams supported by hydro-Quebec and Alcan ALCAN. In: Ibrahimbegovic A, Kozar I (eds) Extreme man-made and natural hazards in dynamics of structures. Springer, Dordrecht, pp 285–309
36. Wang G, Wang Y, Lu W, Yu M, Wang C (2017) Deterministic 3D seismic damage analysis of Guandi concrete gravity dam: a case study. Eng Struct 148(51509182):263–276
37. Omidi O, Valliappan S, Lotfi V (2013) Seismic cracking of concrete gravity dams by plastic–damage model using different damping mechanisms. Finite Elem Anal Des 63:80–97
38. De Falco A, Mori M, Sevieri G, Zani N (2017) Simulation of concrete crack development in seismic assessment of existing gravity dams. In: XVII CONVEGNO ANIDIS "L'Ingegneria Sismica in Italia", Pistoia
39. Lucchesi M, Padovani C, Pasquinelli G, Zani N (2008) Masonry constructions: mechanical models and numerical applications. Springer, Berlin
40. Ansari MI, Agarwal P (2016) Categorization of damage index of concrete gravity dam for the health monitoring after earthquake. J Earthq Eng 20(8):1222–1238
41. Box GE, Tiao GC (1992) Bayesian inference in statistical analysis. Wiley, Hoboken
42. Gardoni P, Der Kiureghian A, Mosalam KM (2002) Probabilistic capacity models and fragility estimates for reinforced concrete columns based on experimental observations. J Eng Mech 128(10):1024–1038
43. Timoshenko S, Goodier JN (1970) Theory of elasticity, 3rd edn. McGraw-Hill College, New York
44. Kang F, Li J, Dai J (2019) Prediction of long-term temperature effect in structural health monitoring of concrete dams using support vector machines with Jaya optimizer and salp swarm algorithms. Adv Eng Softw 131:60–76
45. Azzara RM, De Roeck G, Girardi M, Padovani C, Pellegrini D, Reynders E (2018) The influence of environmental parameters on the dynamic behaviour of the San Frediano bell tower in Lucca. Eng Struct 156:175–187
46. Léger P, Seydou S (2009) Seasonal thermal displacements of gravity dams located in northern regions. J Perform Constr Fac 23:166–174
47. Buffi G, Manciola P, De Lorenzis L, Cavalagli N, Comodini F, Gambi A, Gusella V, Mezzi M, Niemeier W, Tamagnini C (2017) Calibration of finite element models of concrete arch-gravity dams using dynamical measures: the case of Ridracoli. Procedia Eng 199:110–115
48. Tan H, Chopra AK (1995) Earthquake analysis of arch dams including dam–water–foundation rock interaction. Earthq Eng Struct Dyn 24:1453–1474
49. Løkke A, Chopra AK (2013) Response spectrum analysis of concrete gravity dams including dam–water–foundation interaction. Technical report, July
50. Marwala T (2010) Finite element model updating using computational intelligence techniques: applications to structural dynamics, 1st edn. Springer, Berlin
51. Hadamard J (1923) Lectures on Cauchy's problem in linear partial differential equations. Courier Corporation, North Chelmsford
52. Matthies HG, Zander E, Rosić BV, Litvinenko A (2016) Parameter estimation via conditional expectation: a Bayesian inversion. Adv Model Simul Eng Sci 3:1–21
53. Gelman A, Carlin JB, Stern HS, Rubin DB (2004) Bayesian data analysis. Chapman and Hall/CRC, London
54. De Falco A, Girardi M, Pellegrini D, Robol L, Sevieri G (2018) Model parameter estimation using Bayesian and deterministic approaches: the case study of the Maddalena Bridge. Procedia Struct Integr 11:210–217
55. Hariri-Ardebili MA, Seyed-Kolbadi SM, Saouma VE, Salamon J, Rajagopalan B (2018) Random finite element method for the seismic analysis of gravity dams. Eng Struct 171:405–420
56. Rosić B, Matthies HG (2017) Sparse Bayesian polynomial chaos approximations of elasto-plastic material models. In: XIV international conference on computational plasticity. Fundamentals and applications, Barcelona, pp 256–267
57. Sudret B (2008) Global sensitivity analysis using polynomial chaos expansions. Reliab Eng Syst Saf 93(7):964–979
58. Huang Y, Shao C, Wu B, Beck JL, Li H (2018) State-of-the-art review on Bayesian inference in structural system identification and damage assessment. Adv Struct Eng 22:1329–1351
59. MISURE E ANALISI DELLE VIBRAZIONI DIGA DI SCANDARELLO, Technical report, Dipartimento di Protezione Civile: Ufficio Rischio Sismico E Vulcanico Servizio Monitoraggio Sismico Del Territorio Osservatorio Sismico delle Strutture, Ministero delle Infrastrutture e dei trasporti: Dipartimento per le Infrastrutture, i Sistemi Informa. http://www.mot1.it/iss/
60. ISS: Indagini conoscitive e monitoraggi nell'ambito dell'Osservatorio Sismico delle Strutture. http://www.mot1.it/iss
61. ABAQUS, ABAQUS documentation (2014)
62. Lee JH, Fenves GL (1998) Plastic-damage model for cyclic loading of concrete structures. J Eng Mech 124(8):892–900
63. Brooks SPB, Gelman AG (1998) General methods for monitoring convergence of iterative simulations. J Comput Graph Stat 7(4):434–455
64. Sooch GS, Bagchi A (2014) A new iterative procedure for deconvolution of seismic ground motion in dam–reservoir–foundation systems. J Appl Math 2014:287605